



Equilibria and Kinetic Studies on the Adsorption of Cadmium onto Cameroonian Wetland Clays

C. M. Kede^{1,2*}, MA Etoh², P. P. Ndibewu¹, H. M. Ngomo³
and P. M. Ghogomu³

¹Department of Chemistry, Tshwane University of Technology, P.O. Box 56208, 0007 Arcadia, Pretoria, Republic of South Africa.

²Department of Chemistry, Faculty of Science, University of Douala, 00(237)3340 75 69; PO Box 24175 Douala, Cameroon.

³Department of Chemistry, Faculty of Science, University of Yaoundé I, PO Box 812 Yaoundé, Cameroon.

Authors' contributions

This work was carried out in collaboration between all authors. Author CMK designed the study, wrote the first draft and managed the literature searches. Authors PPN and HMN managed all the analysis of the study and corrected the first manuscript. Authors MAE and PMG also corrected the manuscript. All authors read and approved the final manuscript.

Original Research Article

Received 1st April 2013
Accepted 18th November 2013
Published 2nd January 2014

ABSTRACT

The possible use of clay ($Al_2Si_3O_5(OH)_4$, locally mined (Make pe, Cameroon), as an adsorbent, for the removal of cadmium from wastewater was investigated. Spectroscopic studies including FTIR, elemental analysis (EA), XRPD, and SEM were used for its characterization. The effect of different variables, namely: concentration of metal ions, pH and time of interaction were studied. The adsorptive property of clay was tested using Cd(II) as the model adsorbate. Equilibrium data was examined using a comparison of linear isotherm models. The adsorption behavior was well described by the linear Langmuir isotherm model, showing a monolayer adsorption capacity for Cd(II). The kinetic rates were modeled by using the Lagergren-first-order, pseudo-second-order and intra particle model. The pseudo-second-order model was found to explain the adsorption kinetics most effectively. It was also found that the pore diffusion played an important role

*Corresponding author: E-mail: meleack@yahoo.fr, ndibewup@tut.ac.za;

in the adsorption and intraparticle diffusion was the rate-limiting step during the first 30 min. of interaction.

Keywords: Adsorption; kinetic; equilibrium; wetland clays; cadmium.

1. INTRODUCTION

Persistent heavy metal ions in trace quantities are difficult to remove from aqueous solution [1]. Adsorption is a promising technique for regulating mobility of chemical species and their geochemical cycles in the environment. The process has the additional advantages of applicability at very low concentrations, suitable for both batch and continuous processes, ease of operation, little sludge generation, possibility of regeneration and reuse, and low capital cost [2,3]. Thus, adsorption is continuously becoming a preferred method for removal, recovery and recycling of toxic heavy metals from wastewaters. Different types of adsorbents are used for removing metal ions from aqueous solutions [4], each presenting some limitations that may include either cost of the materials or complex chemistry hindering recovery.

Clay minerals are important constituents of soil and they play the role of a natural scavenger for metals as water flows over soils or penetrate underground [1]. By clay standards, kaolinite ($Al_2Si_2O_5(OH)_4$), are the principal constituent of soil nanostructure (up to 40% minerals in sedimentary rocks), [5,6]. The high specific surface area, chemical and mechanical stability, layered structure, high cation exchange capacity (CEC), Brönsted and Lewis acidity, etc., have made the clay minerals excellent materials for adsorption [7]. Mellah and Chegrouche had used bentonite for removing Zn(II) from aqueous solution with Langmuir monolayer capacity of 52.91 mg g^{-1} at 293 K. The adsorption of Cd (II), Cu (II) and Zn(II) on sepiolite has also been reported [8]. Original and Na exchanged bentonites have been used for the removal of Cr(III), Ni(II), Zn(II), Cu(II) and Cd(II) from aqueous solution (Alvarez-Ayuso and Garcia-Sanchez) [9] with maximum adsorption capacity of up to 49.8, 24.2, 23.1, 30.0 and 26.2 mg g^{-1} , respectively. The removal of Cr (III), Cr (VI) and Ag(I) from water by bentonite has also been reported [10] where Cr(III)-bentonite and Ag(I)-bentonite interactions were found to be exothermic while Cr(VI)-bentonite interactions was endothermic.

The present study investigates the adsorption of clay, in batch experiments, for the removal of Cd^{2+} metal ions from aqueous solutions.

2. MATERIALS AND METHODS

2.1 Chemicals

All the chemicals used were of analytical reagent grade. Deionised doubly distilled (DDD) water was used throughout the experimental studies. Working standards were prepared by progressive dilution of stock cadmium solutions (1000 ppm) using the DDD water.

2.2 Materials

The natural clays used in this study was mined from a subtropical wetland soil in Cameroon ((Littoral Region), West Africa. For this type of clay material, the cation exchange capacity (CEC)=12.04 meq/100 g was considered. The specific surface area is $39.824 \text{ m}^2/\text{g}$. The clays

were washed several times with distilled and deionized water after which they were completely dispersed in water. After 17h at rest, the dispersed particles were centrifuged for one hour at 2400 rpm. The size of the clay particles obtained was $0.5 < r < 2 \mu\text{m}$.

These clay particles were dispersed in water and heated at 75°C in the presence of a solution of sodium bicarbonate salts (1.0 M), citrate (0.3 M), and chloride (2.0 M). The purpose of this treatment was to eliminate inorganic and organic compounds, aluminium found in the inter-layer spaces and various free cations [11,12]. Carbonates were removed by treatment with HCl (0.5 M) and chloride was eliminated after several washings. The organic matter was eliminated completely by treatment with H₂O₂ (30% v/v) at 70°C. The purified clay was dried at 110°C, then saturated with sodium (Na⁺). To ensure complete transformation into the sodium form, all samples were washed several times with a NaOH solution (1.0 M).

2.3 Characterization of the Materials

The pH at the potential of zero charge of the clay was measured using the pH drift method. The pH of the solution was adjusted by using 0.01 M sodium hydroxide or hydrochloric acid. Nitrogen was bubbled through the solution at 250°C to remove the dissolved carbon dioxide 10 mg was added to 50 ml of the solution. After stabilization, the final pH was recorded. The graphs of final pH versus initial pH used to determine the zero point charge of the clay [13].

The purity of the natural clay samples was tested by FTIR spectral analysis. An IR transmittance spectrum of the ground samples was obtained in the 4000 to 400 cm⁻¹ range on a PerkinElmer Spectrum Two spectrometer (UK).

To confirm the purity of the natural clay samples, x-ray diffraction (XRD) spectra were obtained. Analysis involved the identification and semi quantification of the characteristic peaks of the minerals present. The XRD diffractograms presented in this study were recorded using a Bruker D8 Discover X-Ray diffractometer (XRD) (UK) from Bruker (Germany) with a D5000 Ni-filtered CuK and an α radiation of 1, 5406 Å. Scans of natural clay samples with both randomly and preferred orientation were taken over a range from $2\theta = 10^\circ$ to 100° at scanning speeds of 0.03°/5 s. The XRD patterns were collected using a Cu K α radiation (1, 5406 Å) source (40 keV, 40 mA). The scans were performed at room temperature in 2θ steps of 0.02°, using open sample holders. The phases were identified using Bruker Diffract Plus evaluation software, distributed by the International Centre for Diffraction Data (ICDD).

Nitrogen adsorption isotherms for pore size distribution and surface area: The adsorbent (IDCA) prepared in this study were analyzed for the specific surface area, pore volume, and PSD by N₂-physisorption using Autosorb-1C instrument (Micromeritics, ASAP 2010). In addition, chemisorption was also carried out to measure the active metal surface area. The multipoint Brunauer, Emmett, and Teller (BET) surface area was measured from the nitrogen adsorption/desorption isotherm. The BET isotherm equation is typically applied on the adsorption isotherm in P/P₀ range of 0.05 to 0.35. Prior to the measurement, the samples were degassed in an out gassing station to remove any adsorbed water or entrapped gases in the IDCA samples. The total pore volume was measured from the amount of vapor adsorbed at the relative pressure close to unity (0.9994).

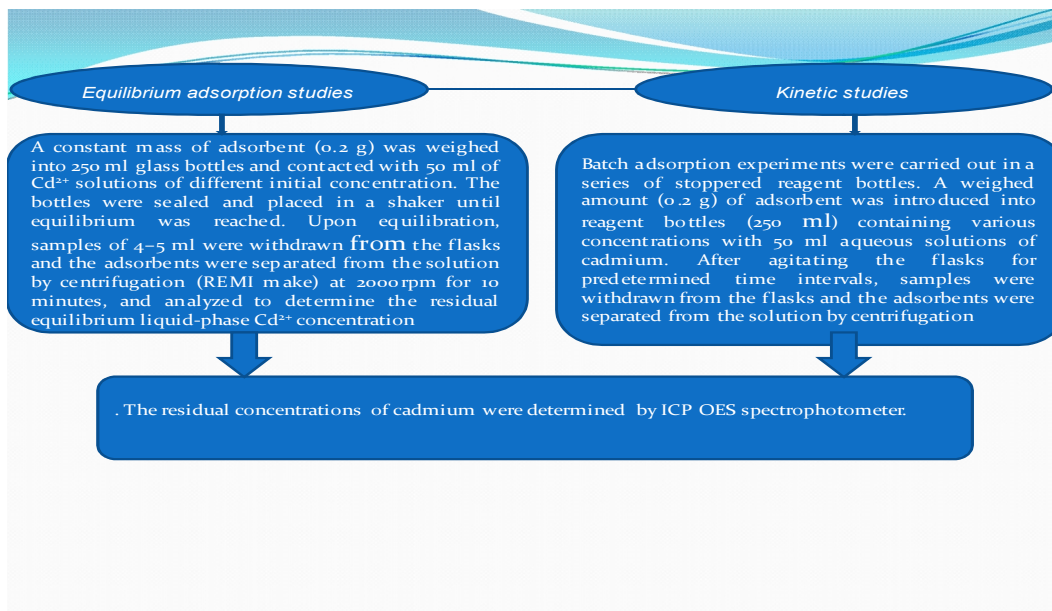
A field emission scanning electron microscopy (FE-SEM) and energy-dispersive x-ray (EDX) was employed to observe the surface morphology of the clay samples. The instrument used

to obtain SEM images and EDX spectra is a JEOL JSM-7600F Field Emission Scanning Electron Microscope, 800 mm², X-Max coupled to a silicon drift energy dispersive X-ray detector (SDD) (Oxford Instruments Ltd, UK).

The samples were gold coated to improve its conductivity so as to obtain good images. Additionally, EDX elemental spectra of a few spots on the samples were taken for determining the surface elemental compositions. Representative images and spectra of the samples are presented in Figs. 3 and 4.

For elemental analysis (EA), the percentage (%) carbon (C), nitrogen (N), oxygen (O) and sulphur (S) of the various samples was equally observed with the EDX spectra, although not very accurate for organic elements.

2.4 Equilibrium Adsorption Studies



The sorption equilibrium data of Cd²⁺ on clay was analyzed using Freundlich and Langmuir isotherm models. Freundlich isotherm equation $x/m = k_f C_e^{1/n}$ can be written in the linear form as given below (1).

$$\log\left(\frac{x}{m}\right) = \log K_F + \frac{1}{n} \log C_e \quad (1)$$

Where x/m (mg/g) and C_e (mg/L) are the equilibrium concentrations of Cd²⁺ in the adsorbed and liquid phases. K_F and n are the Freundlich constants that are related to the sorption capacity and intensity, respectively. Freundlich constants K_F and n can be calculated from the slope and intercept of the linear plot, with $\log(x/m)$ versus $\log C_e$.

The Langmuir sorption isotherm equation $\frac{x}{m} = \frac{Q_{\max} K_L C_e}{1 + K_L C_e}$ on linearization becomes (2)

$$\frac{C_e}{Q_e} = \frac{1}{K_L Q_{\max}} + \frac{1}{Q_{\max}} C_e \quad (2)$$

Where Q_{\max} is the adsorption capacity (mg/g) when all adsorption sites are occupied, C_e is the equilibrium concentration of cadmium, and the Langmuir constant K_L (L/mg) is derived from the ratio of the adsorption rate constant to the desorption rate constant.

2.5 Kinetic Studies

Kinetic adsorption data were analyzed following pseudo-first-order kinetic model:

$$\frac{dq_t}{dt} = k_1(q_e - q_t) \quad (3)$$

Where q_e and q_t refer to the amount of cadmium adsorbed (mg/g) at equilibrium and at any time, t (h), respectively, and k_1 is the equilibrium rate constant of pseudo-first-order sorption (1/h). Integration of Eq. (3) for the boundary conditions $t=0$ to t and $q_t=0$ to q_t , gives

$$\log \frac{q_e}{(q_e - q_t)} = \log q_e - \frac{k_1 t}{2.303} \quad (4)$$

Eq. (4) can be rearranged to give (5)

$$\log(q_e - q_t) = \log q_e - \frac{k_1 t}{2.303} \quad (5)$$

The pseudo second-order model was well-fitted to the Cd^{2+} sorption data on the minerals. The rate equation for the second-order model can be expressed as:

$$\frac{dq_t}{dt} = k_2(q_e - q_t)^2 \quad (6)$$

Where k_2 is the equilibrium rate constant of pseudo-second-order adsorption (g/mg min). Integrating Eq. (6) for the boundary condition $t=0$ to t and $q_t=0$ to q_t , gives (7)

$$\frac{1}{(q_e - q_t)} = \frac{1}{q_t} + k_2 \cdot t \quad (7)$$

which is the integrated rate law for a pseudo-second-order reaction. Eq. (7) can be rearranged to obtain a linear form (8)

$$\left(\frac{t}{q_t}\right) = \left(\frac{t}{q_e}\right) + \left[\left(\frac{1}{k_2 \cdot q_e^2}\right)\right] \quad (8)$$

where, q_t and q_e (mg/g) are the amount of Cd sorbed on the mineral at time t and at equilibrium, respectively and k_2 ($\text{g} \cdot \text{mg}^{-1} \cdot \text{min}^{-1}$) is the second-order rate constant.

2.6 Adsorption Mechanism

In the model developed by Weber and Morris, the rate of intra-particle diffusion is a function of $t^{1/2}$ and can be defined by Eq. (9) as follows:

$$q = f\left(\frac{D_t}{r_p^2}\right)^{1/2} = k_w t^{1/2} \quad (9)$$

Where r_p is particle radius, D_t is the effective diffusivity of solutes within the particle, and K_w intraparticle diffusion rate. k_w values can be obtained by linearizing the curve $q = f(t^{1/2})$.

3. RESULTS AND DISCUSSIONS

3.1 Characterisation of Clay

3.1.1 XRD analysis

In this study the X-ray diffraction patterns of the clay samples were studied. The main aim of XRD study is to observe the influence of Quartz, Kaolinite and Boehmite on the surface of clay. As shown in From (Fig. 1), there are five significant peaks observed at 2θ values (reflection at 4.226 Å, $2\theta = 21.061^\circ$; 2.336 Å, $2\theta = 38.523^\circ$; 1.822 Å, $2\theta = 50.339^\circ$; 1.673 Å, $2\theta = 55.118^\circ$ and 1.377 Å, $2\theta = 68.314^\circ$) which could be attributed to the presence of Quartz. The peaks (reflection at 3.558 Å, $2\theta = 24.973^\circ$; 3.424 Å, $2\theta = 26.775^\circ$; 3.24 Å, $2\theta = 27.676^\circ$; and 2.56 Å, $2\theta = 35.021^\circ$) are assigned to Kaolinite and the peaks (reflection at $d = 1.971 \text{Å}$, $2\theta = 45.835^\circ$ and $d = 1.474 \text{Å}$, $2\theta = 62.589^\circ$) are assigned to Boehmite

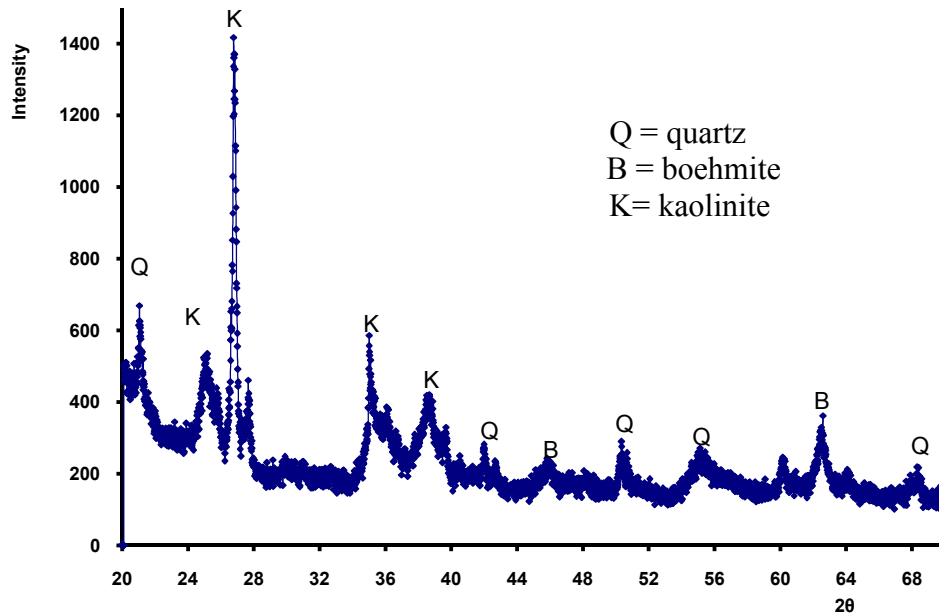


Fig. 1. X-ray diffraction patterns of the natural clay.

3.1.2 Fourier transform-infrared spectroscopy (FTIR)

The FTIR spectrum of the clay is shown in Fig. 2. The frequency absorption band at 3695.8 cm^{-1} (OH-Al out-of-plane), 3624.4 cm^{-1} (OH-Al in-plane) and 913.68 cm^{-1} indicate the presence of OH-Al groups [14].

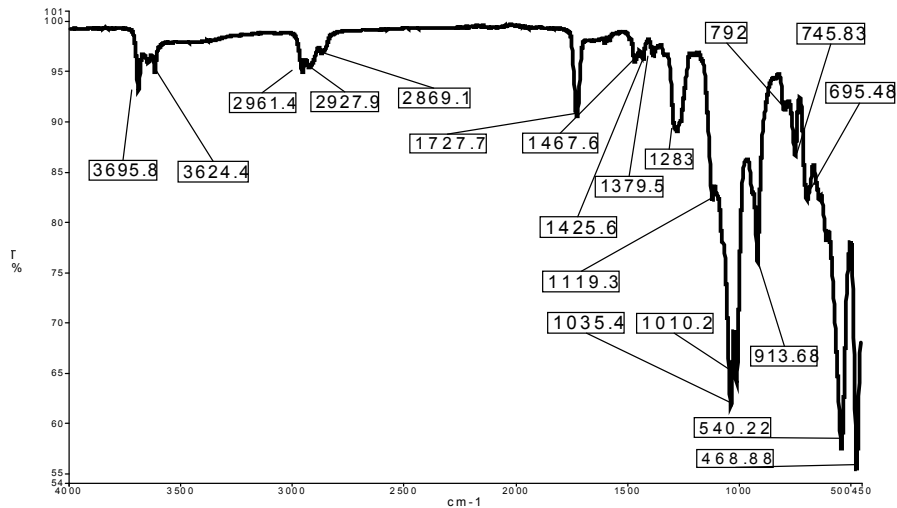


Fig. 2. FTIR spectrum of a sample clay studied (MARV4)

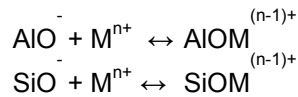
- On one hand, peaks appearing at 2961.4, 2927.9 and 2869.1 cm^{-1} between (2700 and 3150 cm^{-1}) and (1400 and 1500 cm^{-1}) depicts the presence of alkyl groups ($\text{CH}_2\text{-CH}_3$ and CH_3) [15].

- The bands appearing at 1020 and 1120 cm^{-1} are ascribed to the formation of Si - O bond, characteristic of aluminosilicate [16]. The additional peak at 695.45 cm^{-1} indicates the presence of Al-OH and Si-O [16].

- The bands observed at 468.88 and 540. cm^{-1} can be attributed to vibrations due to deformation of Si-O and Si-O-Al bonds, respectively [17].

The groups (OH-Al, Si-O, Si-O-Al) play any important role in cadmium adsorption. This implies that $\text{Cd}(\text{OH})_2$ species may be retained in the micro pores of clay particles by chemisorption involving surface complexes [18]. The functional groups such as (OH-Al, Si-O, Si-O-Al), are assumed to be present on the surface of the clay. When Cd^{2+} is present in the solution the following surface complexes may be formed

- Réaction de formation de complexe de surface:



Avec $\text{M}^{n+} = (\text{Cd}^{2+}, \text{Cd}(\text{OH})^+)$

3.1.3 SEM and EDX

To observe the morphology of the clay sample, an example of a scanning electron microscopy (SEM) image is shown in Fig. 3. The image displays the SEM micrographs of functionalized clay. In this case, the particles are apparently smaller in size than natural clay sample and are composed of disordered thin sheet particles aggregates. One can conclude that functionalization promotes the formation of disordered and less cohesive aggregates, probably due to a reduction of the edge-to-edge and face-to face interactions. Unlike the hydrophilic end, which formed large size aggregates after drying of the clay sample became hardened and dispersed in water (hydrophobic) while easily kept as a loose powder after drying. This change constitutes an important advantage considering the product application in commercial units. The EDX plot (Fig. 4) of clay shows the presence of carbon, oxygen, and inorganic elements like aluminium, titanium, silicon, zinc, copper and iron (Table 1).

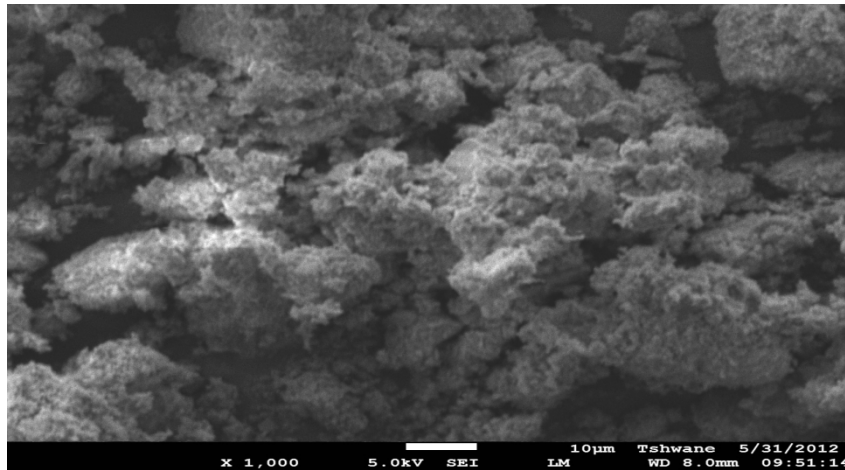


Fig. 3. SEM photographs of a sample clay sample (MARV4)

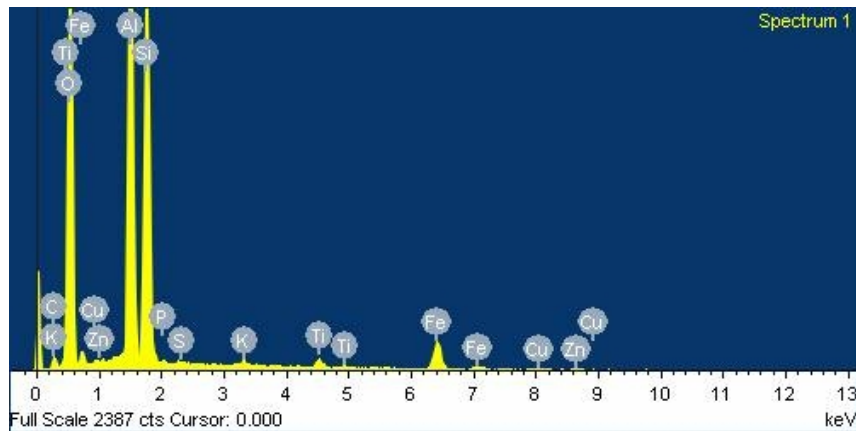


Fig. 4. EDX of a sample clay sample MARV4 showing abundance of certain metals (Al and Si are typically present in clay minerals of this type)

Table 1. Elemental Analysis of Clay

Elements	C	O	Al	Si	P	S	K	Ti	Cu	Fe	Zn
Weight%	4.36	62.27	14.01	14.51	0.17	0.01	0.15	0.52	0.24	3.11	0.55
Atomic%	6.70	72.49	9.60	9.56	0.10	0.01	0.07	0.20	0.07	1.03	0.15

3.2 Effects of Contact Time and Initial Concentration of Cd²⁺

The effect of contact time on batch adsorption of initial Cd²⁺ concentration ranged from 10 to 60 ppm at room temperature is shown in Fig 5. The amount of adsorption increases rapidly in the beginning and then gradually increases to reach an equilibrium value in 60 minutes. The increase in uptake capacity of the adsorbent with increasing Cd²⁺ concentration may be due to higher probability of collision between Cd²⁺ ions and adsorbent particles. The variation in the extent of adsorption may also be due to the fact that initially all sites on the surface of adsorbent were vacant and the solute concentration gradient was relatively high.

Consequently, the extent of Cd^{2+} uptake decreases significantly with the increase of contact time, which is depending on the decrease in the number of vacant sites on the surface. This data is important because equilibrium time is one of the parameters for economic feasibility studies for in wastewater treatment plant application [19]. According to these results, the agitation time was fixed at 2h for the rest of the batch experiments to make sure that equilibrium was attained.

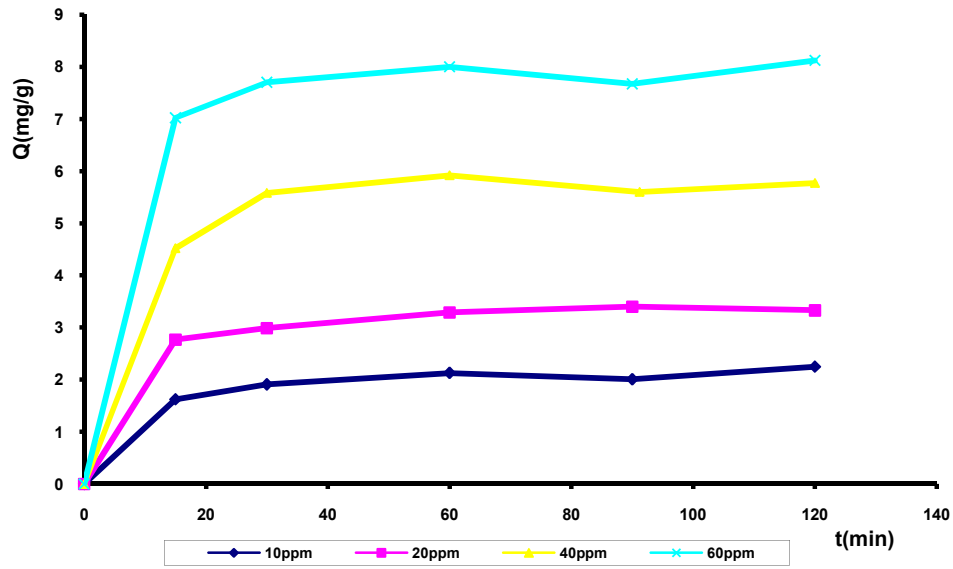


Fig. 5. Effect of agitation time and initial concentration of Cd^{2+} on the adsorption of Cd^{2+} clay concentration, 0.2g/50 mL.)

3.3 Effect of pH

The pH of the aqueous solution is an important parameter which controls the sorption process [20] and metal removal typically increases with increasing pH values [21]. The pH may affect the ionization degree of the sorbate and the surface properties of the sorbent [22]. Chemically, the solution pH influences metal speciation. For instance, heavy metal ions may form complexes with inorganic ligands such as OH. The extent of the complex formation varies with pH, the ionic composition and the particular metal concerned. Exposure of clay surface to water causes the ionization of surface hydroxyl groups (OH-Al, Si-O, Si-O-Al). The degree of ionization depends on pH, and the acid/base reaction occurring at the hydroxyl groups may results in surface charge development [23]. Clays are not only influenced by pH but in turn are capable of affecting solution pH especially in batch system [24] and clays tend to have a higher internal pH. In addition, the clay surface may be influenced by the ambient pH which is not equal to the external solution pH value and precipitation within the channels of clay and at the surface of clay may occur. The effect of the solution pH on the removal of Cd^{2+} ions by clay was examined. Based on the solubility product of metal hydroxides [25] the pH of precipitation at the tested concentration was plotted as illustrated in Fig.6, the pH values were varied from 2 to 12 through this experiment. The maximum adsorption for Cd^{2+} was found at pH of 6.7. It is clear from the presented figure that the removal of metal ions is a pH dependent process. The adsorption mechanism on clay surfaces reflected the nature of the physicochemical interaction of the metal ions in solution and the active sites of clay [26].

The low acidity (pH below 4) may collapse clay structure, especially that with low Si/Al ratio, but the destruction will be more at pH below 3. Biskup and Subotic 2004, stated that pH below 4.5 is not recommended for clay. Therefore, the decrease in removal capacity at low pH can be attributed to the collapse of clay structure. Out of these reasons and depending on the results of Fig. 6 an optimum pH of 6.7 was suggested to carry out the adsorption experiments.

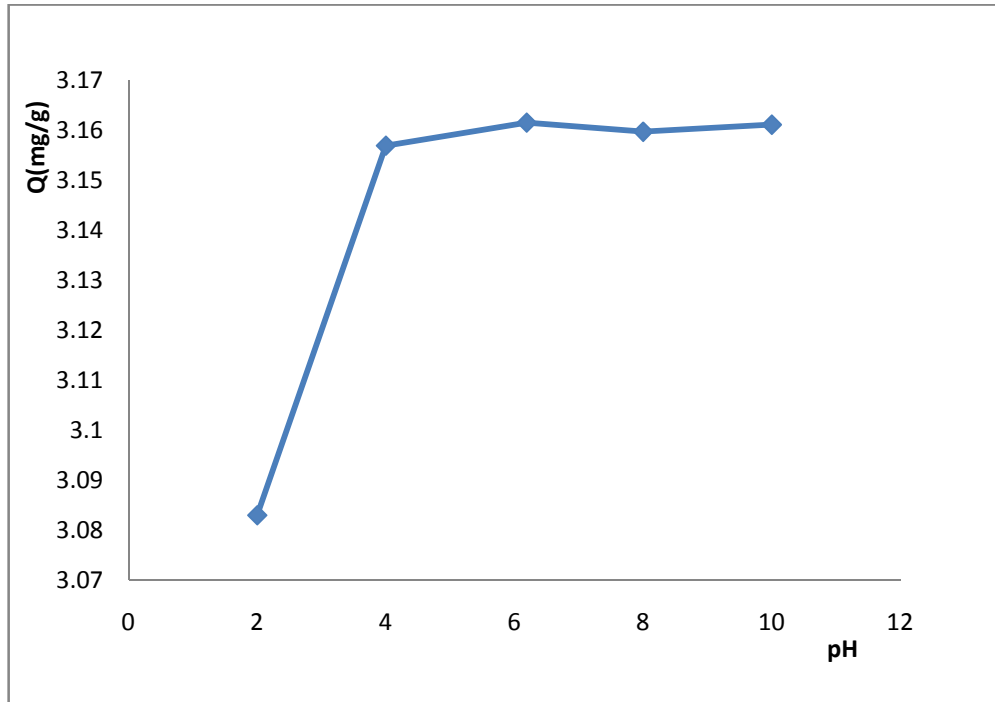


Fig. 6. Effect of pH on removal of cadmium (initial concentration 10 mg/l; contact time 120 min)

3.3 Equilibria Isotherms

The analysis of the isotherm data is important to develop an equation which accurately represents the results and could be used for designing purposes. The sorption data was analysed in terms of Freundlich and Langmuir isotherm models. The fitted constants for Freundlich and Langmuir models along with regression coefficients are summarised in Table 2. The Freundlich and Langmuir isotherms are shown graphically in Figs. 7 and 8. As can be seen from isotherms and regression coefficients, the fit is better with Langmuir model than with Freundlich model. The Langmuir constants Q_m and K_L were 13.869 mg/g and 0.036 for cadmium. The essential characteristics of the Langmuir isotherm can be expressed in terms of a dimensionless constant separation factor or equilibrium parameter, R_L , which is defined

$$\text{as } R_L = \frac{1}{1 + K_L C_0}$$

where K_L is the Langmuir constant and C_0 is the initial concentration of Cd^{2+} . The R_L value indicates the shape of the isotherm as follows.

$R_L > 1$ Unfavourable

$R_L = 1$ Linear

$0 < R_L < 1$ Favourable

$R_L = 0$ Irreversible

Table 2. Isotherm parameters for cadmium adsorption onto clay

Langmuir	Q_{max} (mg/g)	K_L (L/mg)	R^2
	13.869	0.036	0.982
Freundlich	K_f (mg/g)	n	R^2
	1.647	2.411	0.634

According to Mckay et al. 1982. R_L values between 0 and 1 indicate favourable adsorption. The R_L value for cadmium was 0.31, for concentration of 60 ppm. Hence, the adsorption of the metal ions on clay seems to be favourable. The Freundlich constants K_F and n were 1.647, 2.411 for cadmium, respectively. It has been shown that 'n' values between 1 and 10 represent beneficial adsorption.

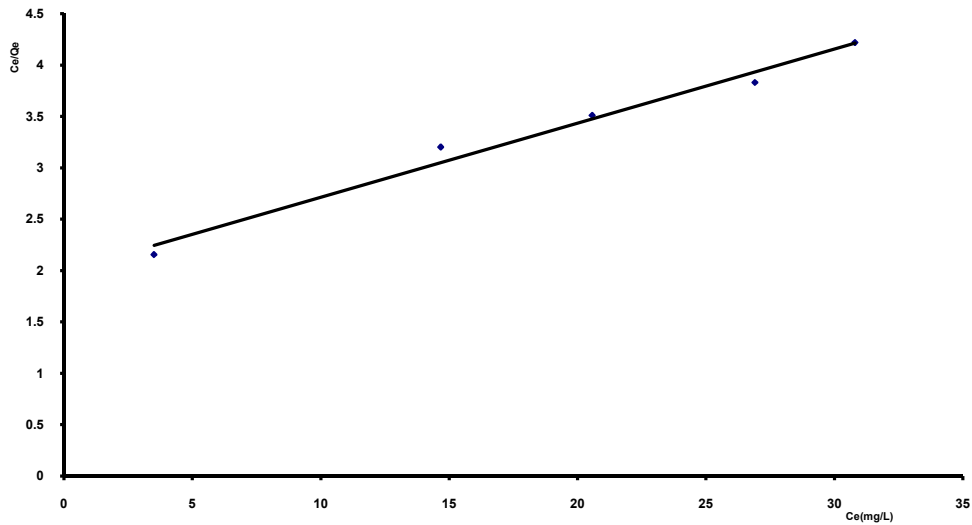


Fig. 7. Langmuir isotherm for cadmium adsorption onto clay at room temperature

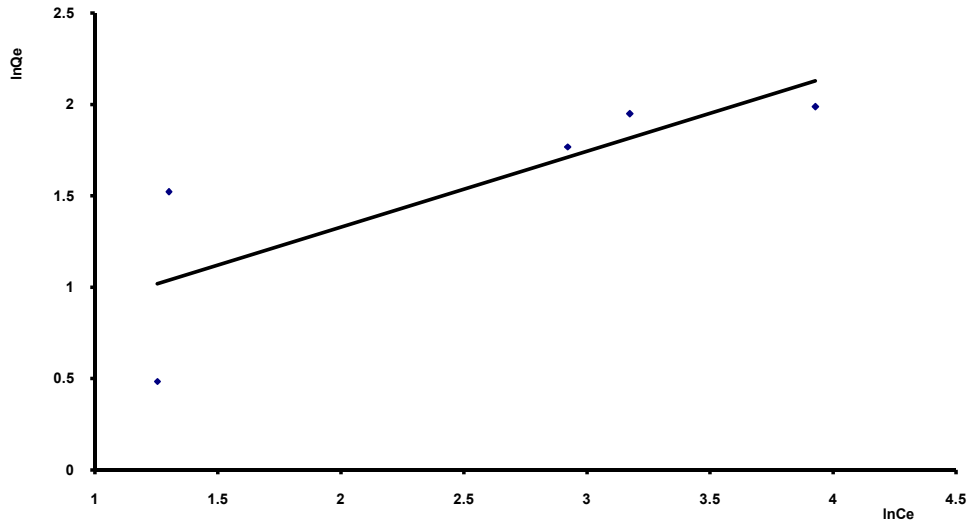


Fig. 8. Freundlich isotherm for cadmium adsorption onto clay at room temperature

3.4 Kinetic Studies

In order to investigate the kinetics of adsorption of Cd^{2+} , the Lagergren-first-order model and Ho's pseudo-second-order model [27,28,29] were used. The values of the parameters and the correlation coefficients obtained using linear regression by origin version 7.0 at four concentrations are listed in Table 3. Adsorption equation obtained and the fitting of the kinetic models are illustrated in Figs. 9-10. It was found that the fitting to Ho's pseudo-second-order model gave the highest values of correlation coefficients more accurately than the other two models investigated. Therefore, Ho's pseudo-second-order model could be used for the prediction of the kinetics of adsorption of Cd^{2+} on clay.

Table 3. Kinetic parameters for Cd^{2+} adsorption onto clay

Model	Lagergren		2 nd order			Intraparticulaire diffusion		
	K_1 (min^{-1})	R^2	K_{2app} ($g.mg^{-1}.min^{-1}$)	R^2	$h(mg.g^{-1}.min^{-1})$	K_w	R^2	t
10 ppm	0.002	0.611	0.111	0.999	0.350	0.106	0.240	2.019
20 ppm	0.009	0.861	0.074	0.999	0.894	0.099	0.856	1.299
40 ppm	0.017	0.748	0.064	0.997	2.240	0.088	0.607	0.790
60 ppm	0.020	0.994	0.113	0.996	6.635	0.028	0.946	0.366

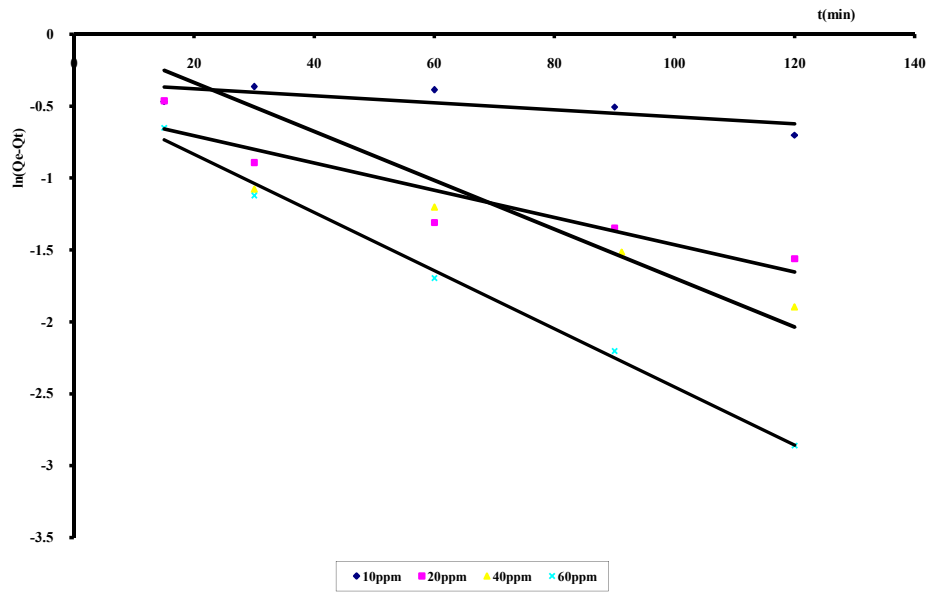


Fig. 9. Pseudo-first-order kinetics for adsorption of Cd^{2+} onto clay

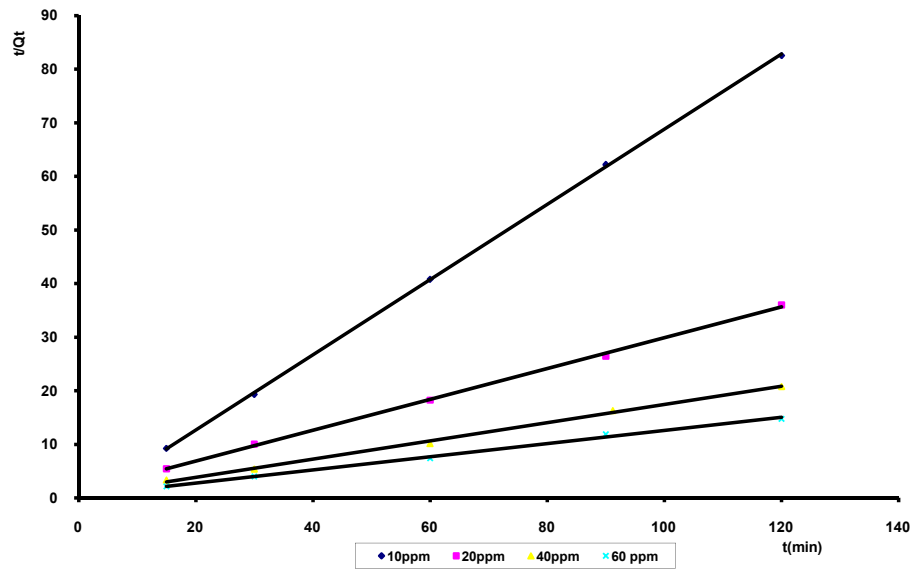


Fig. 10. Pseudo-second-order kinetics for adsorption of Cd^{2+} onto clay

The values of the initial adsorption rate were found to increase from 0.350 to 6.635 for increase in the initial Cd^{2+} ion concentration from 10 to 60 mgL^{-1} . As for the other two models, it is not clear that there is a second best; Lagergren's model performs reasonably well at high Cd^{2+} concentration and the goodness of fit deteriorates.

3.5 Adsorption Mechanism

The intra-particle diffusion rates (K_w) were determined using linear regression. If intra-particle diffusion is a rate controlling step, then the plots should be linear and pass through the origin. In most cases these plots give general features of three stages; initial curved portion, followed by an intermediate linear portion and a plateau. The initial portion due to external mass transfer, the intermediate linear part is due to intra-particle diffusion and the plateau to the equilibrium stage where intraparticle diffusion starts to slow down due to extremely low solute concentrations in the solution. A plot of the quantity of the cation adsorbed against 15min is shown in Fig. 11. It can be observed that the plots are not linear over the whole time range and the graphs of this figure reflect a dual nature, with initial linear portion followed by plateau. This implies that the external surface adsorption (stage 1) is absent and the stage of intra-particle diffusion (stage 2) is attained and continued to 90 min. Finally, equilibrium adsorption (stage 3) starts after 90 min. The cations are slowly transported via intra-particle diffusion into the particles and are finally retained in the pores. Similar dual nature of intraparticle diffusion curve with initial linear portion was found for adsorption of phosphorus onto calcined alunite [30,31]. The rates constants of intra-particle diffusion were calculated using linear regression and were found to be 0.106, 0.099, 0.088 and 0.028 mg/g.min for Cd^{2+} . However, the linear portion of the curve does not pass the origin and the latter stage of cadmium adsorption does not obey Weber–Morris equation. It may be concluded that the adsorption mechanism of this cation from aqueous solution is rather complex process and the intra-particle diffusion was not the only rate-controlling step.

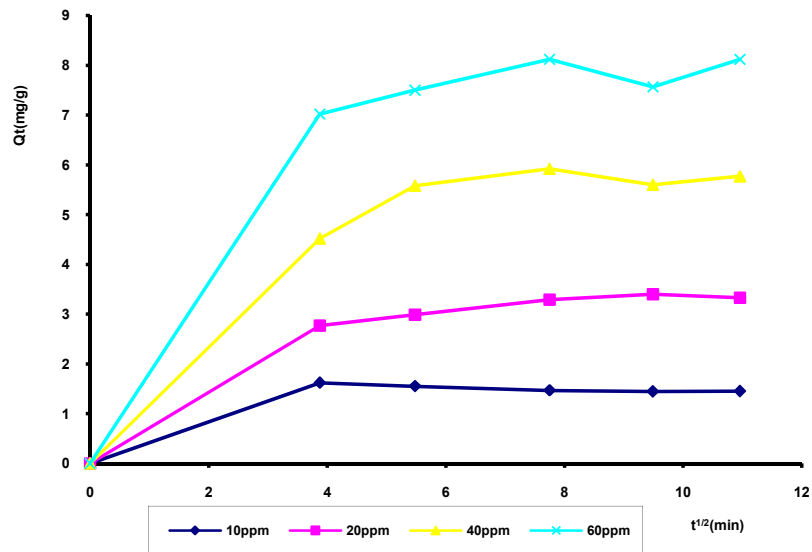


Fig. 11. Plot of intraparticle diffusion model for adsorption of Cd^{2+} on clay

4. CONCLUSIONS

The present investigation showed that the clay used as an adsorbent can be effective for the removal of Cd^{2+} from dilute aqueous solution. The adsorption amount increased with increasing concentration. The maximum adsorption capacity was found to be 13.869 mg/g of clay. The Langmuir and Freundlich isotherm equations were used to interpret the adsorption phenomenon of the adsorbate, and the Langmuir isotherm was found to best describe the experimental data. There are several factors affecting the adsorption of metal ions onto clay. The kinetic rates were modelled using the Lagergren-first-order and pseudo-second-order equations, and the pseudo-second-order equation was found to explain the adsorption kinetics most effectively. It was also found that the pore diffusion played an important role in the adsorption. From an analytical point of view, spectroscopic techniques (XRD and FT-IR) and electron microscopy coupled to x-ray dispersive elemental surface analysis (SEM/EDs) were found to be powerful tools for the characterization of clay materials.

ACKNOWLEDGEMENTS

This research was supported by the Universities of Yaoundé I and Douala, both in Cameroon. Appreciation is expressed to the Academy of Sciences for the Developing World (TWAS) in Trieste, Italy, for financial assistance to the main author to travel to the host institution, the Tshwane University of Technology (TUT), in Pretoria, South Africa working under Profs RI McCrindle & PP Ndibewu. Finally, the National Research Foundation (NRF) of South Africa is acknowledged for having provided funds to the host institution (TUT) necessary for the procurement of chemicals used throughout the entire project.

COMPETING INTERESTS

Authors have declared that no competing interests exist.

REFERENCES

1. Krishna G Bhattacharyya, Susmita Sen Gupta. Kaolinite and montmorillonite as adsorbents for Fe(III),Co(II) and Ni(II) in aqueous medium. *Applied Clay Science*. 2007;41;1–9
2. Yavuz O, Altunkaynak Y, Guzel Y. Removal of copper, nickel, cobalt and manganese from aqueous solution by kaolinite. *Water Res*. 2003;37:948–952.
3. Saleh Kaoser, Suzelle Barrigton, Maria Elektorowicz, Li Wang Effect of Pb^{2+} and Cd^{2+} on Cu^{2+} by bentonite liners. *Can.J civ. Eng*. 2005;32:241-249.
4. Alvarez-Ayuso E, Nugteren HW. Purification of chromium (VI) finishing wastewaters using calcined and uncalcined Mg–Al– CO_3 –hydrotalcite. *Water Res*. 2005;39:2535–2542.
5. Ndibewu PP, Mgangira. MB, Cingo N, McCrindle RI. Metal and anion composition of two biopolymeric chemical stabilizers and toxicity risk implication for the environment. *Journal of Toxicology and Environmental Health, Part A*. 2010;73(4);261-271.
6. Pedra F, Polo. A, Ribeiro A, Domingues H. Effects of municipal solid waste compost and sewage sludge on mineralization of soil organic matter. *Soil Biology and Biochemistry*. 2007;39(6):1375–1382.
7. Tanabe K. Catalysis—science and technology. In: Anderson, JR Boudart, M(Eds.), Springer-Verlag, New York. 1981;231.

8. Sanchez AG, Ayuso EA, De BOJ. Sorption of heavy metals from industrial wastewater by low cost mineral silicates. *Clay Miner.* 1999;34:469–477.
9. Alvarez-Ayuso E, Garcia-Sanchez A. Removal of heavy metals from waste waters by natural and Na-exchanged bentonites. *Clays Clay Miner.* 2003;51:475–480.
10. Khan SA, Rehman R, Khan MA. Adsorption of chromium (III), chromium (VI) and silver (I) on bentonite. *Waste Manag.* 1995;15:271–282.
11. Bouras O, Khalaf H, Houari M, Moustiri F. The adsorption of the textile colorants thio acid pink and violet cibacete by algerian bentonite, Jordan International Chemical Engineering Conference III, Amman (Jordan).1999;225-241.
12. Khalaf H, Bouras O, Perrichon V. Synthesis and characterisation of Alpillared and cationic surfactant modified Algerian bentonite, *Microporous Mater.*1997;8:141-150.
13. Lopez-Ramon MV, Stoeckli F, Morenco-Castilla C, Carrasco-Martin F. On the caracerization of acidic and basic surface site on carbons by various techniques. *Carbon.* 1999;37:215-1221.
14. Farmer VC. The Layer Silicates: The Infrared Spectra of Minerals. In: V.C. Farmer (Ed.), *Mineralogical Society*, London.1974;4:331–363.
15. Bouras O, Propriétés Adsorbantes d'Argiles Pontées Organophiles :Synthèse et Caracterisation ; 2003.
16. Amritphale SS, Bhasin S, Chandra N. Energy Efficient Process for Making Pyrophyllite-based Ceramic Tiles Using Phosphoric Acid and Mineralizes. *Ceramics International*, Article in press; 2005.
17. Sayilkan H, Erdemoglu S, Sener S, Sayilkan F, Akarsu M, Erdemoglu M, Surface Modification of Pyrophyllite with Amino Silane Coupling Agent for the Removal of 4-Nitrophenol from Aqueous Solutions. *Journal of Colloid and Interface Science.* 2004; 275:530–538.
18. Kadirvelu K, Namasivayam C. *Adv. Environ. Res.* 2003;7:471.
19. Yardim MF, Budinova T, Ekinci E, Petrov N, Razvigorova M, Minkova V, Removal of Mercury (II) from Aqueous Solution by Activated carbon obtained from Furfural', *Chemosphere.* 2003;52:835–841
20. Elliott HA., Huang CP. Adsorption characteristics of some Cu(II) complexes on aluminosilicates, *Water Res.* 1981;15:849-855.
21. Leinonen H, Lehto J. Purification of metal finishing waste waters with zeolites and activated carbons, *Waste Manage. Res.* 2001;19:45-57.
22. Motsi T., Rowson NA, Simmons MJH. Adsorption of heavy metals from acidmine drainage by natural zeolite, *Int. J. Miner. Process.* 2009;92:42-48.
23. Hui K.S, Chao CYH, Kot SC. Re-moval of mixed heavy metal ions in wastewater by zeolite 4A and residual products from re-cycled coal fly ash. *Journal of Hazardous Materials B.* 2005;127:89-101.
24. Lin CY, Yang DH. Removal of pollutants from wastewater by coal bottom ash, *J. En-viron. Sci. Health, Part A: Toxic/Hazard. Subst. Environ. Eng.* 2002;37:1509-1522.
25. Covarrubias CR, Arriagada J, Yanez R, Garcia M, Angelica SDB arros, Arroyo P, Sousa-Aguiar EF. Removal of chromium (III) from tannery effluents, using a system of packed columns of zeolite and activated carbon, *J.Chem.Technol. Biotechnol.* 2005; 80;899-908.
26. Misaelides P. Application of natural zeolites in environmental remediation: A short review. *Microporous and Mesoporous Materials.* 2011;144:15-18.
27. Ho YS, McKay G. The Kinetics of Sorption of Divalent Metal Ions onto Sphagnum Moss Peat', *Water Research.* 2000;34(3):735-742.
28. Wu P, Wu W, Li S, Xing N, Zhu N, Li P, Wu J, Yang C, Dang Z. Removal of Cd²⁺ from aqueous solution by adsorption using Fe-montmorillonite. *J. Hazard. Mater.* 2009;169. 824-830.

29. Zhau G, Wu X, Tan X, Wang X. Sorption of heavy metal ions from aqueous solutions: A review. *Open Colloid Sci. J.* 2011;4:19-31.
30. Ozacar M. Equilibrium and kinetic modelling of adsorption of phosphorus on calcined alunite, *Adsorption.* 2003;9:125–132.
31. Daifullah AAM, Yakout SM, Elreefy SA. Adsorption of fluoride in aqueous solutions using KMnO₄-modified activated carbon derived from steam pyrolysis of rice straw. *Journal of Hazardous Materials.* 2003;147:633–643.

© 2014 Kede et al.; This is an Open Access article distributed under the terms of the Creative Commons Attribution License (<http://creativecommons.org/licenses/by/3.0>), which permits unrestricted use, distribution, and reproduction in any medium, provided the original work is properly cited.

Peer-review history:

The peer review history for this paper can be accessed here:
<http://www.sciencedomain.org/review-history.php?iid=384&id=5&aid=2945>